



HAL
open science

Anti-CD160, Alone or in Combination With Bevacizumab, Is a Potent Inhibitor of Ocular Neovascularization in Rabbit and Monkey Models

Thierry Menguy, Anne Briaux, Elisabeth Jeunesse, Jérôme Giustiniani, Alexandre Calcei, Thierry Guyon, Jacques Mizrahi, Hélène Haegel, Vanessa Duong, Vincent Soler, et al.

► **To cite this version:**

Thierry Menguy, Anne Briaux, Elisabeth Jeunesse, Jérôme Giustiniani, Alexandre Calcei, et al.. Anti-CD160, Alone or in Combination With Bevacizumab, Is a Potent Inhibitor of Ocular Neovascularization in Rabbit and Monkey Models. *Investigative Ophthalmology & Visual Science*, 2018, 59 (7), pp.2687-2698. 10.1167/iovs.18-24024 . hal-03379522

HAL Id: hal-03379522

<https://ut3-toulouseinp.hal.science/hal-03379522>

Submitted on 15 Oct 2021

HAL is a multi-disciplinary open access archive for the deposit and dissemination of scientific research documents, whether they are published or not. The documents may come from teaching and research institutions in France or abroad, or from public or private research centers.

L'archive ouverte pluridisciplinaire **HAL**, est destinée au dépôt et à la diffusion de documents scientifiques de niveau recherche, publiés ou non, émanant des établissements d'enseignement et de recherche français ou étrangers, des laboratoires publics ou privés.

Anti-CD160, Alone or in Combination With Bevacizumab, Is a Potent Inhibitor of Ocular Neovascularization in Rabbit and Monkey Models

Thierry Menguy,¹ Anne Briaux,² Elisabeth Jeunesse,³ Jérôme Giustiniani,⁴⁻⁷ Alexandre Calcei,¹ Thierry Guyon,⁸ Jacques Mizrahi,¹ Hélène Haegel,¹ Vanessa Duong,¹ Vincent Soler,⁹⁻¹¹ Pierre Brousset,¹² Armand Bensussan,⁴ Isabelle Raymond Letron,³ and Philippe Le Bouteiller^{2,4}

¹Elsalys Biotech, Lyon, France

²Centre de Physiopathologie de Toulouse Purpan, INSERM UMR 1043, CNRS UMR 5282, Université Toulouse III, Toulouse, France

³STROMALab, Université de Toulouse, EFS, ENVT, INSERM U1031, Toulouse, France et LabHPEC, Ecole Nationale Vétérinaire, Toulouse, France

⁴INSERM UMR 976, Hôpital Saint-Louis, Paris, France

⁵Université Paris Diderot-Paris 7, Paris, France

⁶Institut Jean Godinot, Unicancer, F-51726 Reims, France

⁷Université Reims-Champagne-Ardenne, DERM-I-C, EA7319, Reims, France

⁸Mabsolys, Evry, France

⁹Unité de Rétine, Ophthalmology Department, Hôpital Pierre-Paul Riquet, Toulouse University Hospital, Place Baylac, Toulouse, France

¹⁰Unité Différenciation Epithéliale et Autoimmunité Rhumatoïde UMR 1056 Inserm - Université Toulouse III, Toulouse, France

¹¹Université Toulouse III, Toulouse, France

¹²Centre de Recherche en Cancérologie de Toulouse, INSERM UMR1037, Toulouse, France

Correspondence: Thierry Menguy, Elsalys Biotech 317 avenue Jean Jaurès, 69007 Lyon, France; Menguy@elsalysbiotech.com.

AB, IRL, and PLB contributed equally to the work presented here and should therefore be regarded as equivalent senior authors.

Submitted: February 3, 2018

Accepted: April 24, 2018

Citation: Menguy T, Briaux A, Jeunesse E, et al. Anti-CD160, alone or in combination with bevacizumab, is a potent inhibitor of ocular neovascularization in rabbit and monkey models. *Invest Ophthalmol Vis Sci*. 2018;59:2687-2698. <https://doi.org/10.1167/iovs.18-24024>

PURPOSE. To assess the efficacy of the murine first-in-class CL1-R2 monoclonal antibody (mAb) targeting human CD160 (alone or in combination with bevacizumab) by using the rabbit corneal neovascularization (CNV) model, and determine the safety and efficacy of ELB01101, a novel CL1-R2-derived humanized IgG4 mAb, in a monkey model of choroidal neovascularization (ChNV).

METHODS. Comparison of effect of CL1-R2, bevacizumab, or aflibercept or IgG1 (control) injections in early and late treatment schemes on evolution of VEGF- or FGF2-induced rabbit CNV was performed. In the combination setting, bevacizumab was coinjected with different doses of CL1-R2. ELB01101 or vehicle was administered intravitreally in monkeys after laser-induced ChNV. Individual laser-induced lesions were semiquantitatively graduated by using fluorescein angiography to determine leakage.

RESULTS. In the rabbit model, early and late treatments with CL1-R2 significantly decreased both area and length of CNV neovessels. The effect was as potent as produced with anti-VEGF comparators. When combined with bevacizumab, an additive effect of CL1-R2 was measured at all doses tested. In the ChNV model, on day 29, eyes treated with ELB01101 showed a statistically significant reduction in clinically relevant lesions compared to vehicle-treated eyes (~50%; χ^2 test, $P = 0.032001$).

CONCLUSIONS. The additive effects of anti-CD160 and bevacizumab in the CNV model suggest that these compounds could act via different pathways, opening new therapeutic pathways for cotargeted or combination therapies. In the ChNV model, ELB01101 was well tolerated and prevented approximately 50% of clinically relevant lesions, validating CD160 targeting as a safe approach for treatment of retinal diseases in the most relevant animal model of wet AMD.

Keywords: CD160, monoclonal antibody, anti VEGF, neovascularization, combotherapy

Angiogenesis, the formation of new blood vessels from preexisting vasculature, is a physiological process.¹ However, it also plays a role in a number of diseases, including corneal/retinal neovascular diseases—mainly ischemic retinopathies (IRs) or choroidal retinopathies such as exudative or “wet” age-related macular degeneration (wAMD).² Together, these diseases constitute the primary cause of moderate and severe vision loss in developed countries.^{3,4}

Increasing knowledge of angiogenesis and its etiology in wAMD and IRs has led to the development of drugs targeting the VEGF (vascular endothelial growth factor) pathway. Intravitreal (IVT) injections of anti-VEGF therapeutic agents have been used over the past decade as the first line of treatment for wAMD,⁵ retinal vein occlusion, and macular edema.^{6,7}



Even though anti-VEGF therapy appears safe in the general population, several practical limitations related to its efficacy have emerged, including the high cost of some agents and the need for frequent IVT injections in many cases to reach full efficacy. Indeed, even with regularly repeated anti-VEGF therapy over 1 year, approximately a third of wAMD patients respond poorly or not at all to anti-VEGF agents with standard treatment, or they present reduced long-term efficacy.⁸ Approximately 20% of patients lose vision, around 50% fail to achieve 20/40 visual acuity (VA), and two-thirds achieve a VA gain of fewer than three ETDRS lines.^{9,10} Consequently, up to 30% of patients treated with anti-VEGF therapies are considered resistant to the treatment or to have refractory neovascular AMD, as defined in the study of Yang et al.¹¹ A number of causes have been suggested for this disappointing outcome, such as misdiagnosis, redundancy of proangiogenic pathways, genetic AMD risk variants, tachyphylaxis, or tolerance to current anti-VEGF therapies.¹¹⁻¹⁴

These limitations underline the need to improve sustained delivery approaches for anti-VEGFs without increasing the induction of tolerance or raising safety issues while also reducing the number of injections required. For patients responding incompletely to anti-VEGF therapy, it would be beneficial to be able to target other molecules involved in angiogenesis and/or inflammation; thus there is a pressing need to develop VEGF-independent complementary and synergistic therapies that inhibit pathologic neovascularization while having little or no effect on normal mature tissue vasculature.

Our previous results indicate that, *in vitro*, specific engagement of the hCD160 receptor on activated endothelial cells by the CL1-R2 agonist, a murine mAb, inhibits fibroblast growth factor 2 (FGF2)-mediated tubule vessel growth from HUVECs (human umbilical vein endothelial cells) expressing CD160.¹⁵ Antiangiogenic therapeutic efficacy of CL1-R2 has been shown *in vivo* in a number of animal models of ocular and tumor neovascularization, results that support the relevance of this mechanism of action for ocular diseases. Indeed, CL1-R2 inhibits retinal neovascularization in a mouse model of oxygen-induced proliferative retinopathy (ROP model), choroidal neovascularization (ChNV) in a murine model of wAMD, and FGF2-induced ocular neovascularization in a rabbit corneal neovascularization (CNV) model.¹⁶ Furthermore, CL1-R2 treatment of B16 tumoral vascularization in mice blocks neoangiogenesis and normalizes the structure of the remaining vessels.¹⁶

In healthy tissues expression of CD160, also known as BY55, is restricted to the spleen, small intestine, normal cytotoxic peripheral blood natural killer (NK) cells (CD56^{dim} CD160⁺ subset), circulating T-lymphocyte subsets,¹⁷⁻²⁰ some mast cells (MCs),²¹ and the CD163^{high}-CD160^{high} subset of anti-inflammatory mononuclear phagocytes.²² Cleavage of the glycosylphosphatidylinositol (GPI) anchor by phospholipase D has been shown to cause release of a trimeric soluble form of CD160 (sCD160) from activated NK cells²³ or by MCs.²¹

Several recent reports indicate that subconjunctival administration of bevacizumab or ranibizumab anti-VEGF mAbs inhibits CNV in rabbits.^{24,25} Bevacizumab prevents CNV more effectively when the treatment is applied early rather than late.²⁴ The CNV rabbit model is now recognized as a standard model for preclinical studies comparing the effects of new compounds with those of other antiangiogenic agents.

Laser-induced ChNV in monkeys has become the gold standard for the clinical evaluation of antiangiogenic and anti-inflammatory drugs used to treat ocular neovascular diseases. This model has been extensively used to assess the efficacy of a number of anti-VEGF drugs²⁶⁻²⁹ and demonstrates good

translational predictability for human clinical studies of treatments for retinal diseases.

In this study, the efficacy of the parental CL1-R2 anti-CD160 mAb delivered as subconjunctival injections early and late in the rabbit CNV model was assessed. The results provide additional qualitative and quantitative information on the efficacy and potency of CL1-R2 for the inhibition of CNV in the rabbit experimental model. CL1-R2 was used as a stand-alone treatment and compared to bevacizumab (mAb) or aflibercept (fusion protein, reference treatment for wAMD) anti-VEGF agents, as well as in combination with bevacizumab.

We also assessed the efficacy and tolerance of ELB01101, a novel CL1-R2-derived humanized therapeutic anti-CD160 IgG4, in the nonhuman primate (NHP) experimental model of laser-induced ChNV. The results from this relevant preclinical model demonstrated that anti-CD160 therapy could be used as a main player in future treatment of neovascular ocular diseases.

MATERIALS AND METHODS

Antiangiogenic Agents Used in Animal Models

The murine IgG1 CL1-R2 mAb targeting human CD160 was as described.^{15,16} CL1-R2 is defined by the sequences reported in patent EP1776387B1 and was produced from the I-3204 hybridoma (available from the Collection Nationale de Cultures de Microorganismes [CNCM] depository). CL1-R2 was purified by passage on protein G Sepharose 4 Fast Flow (17-0618-01; GE Healthcare, Pittsburgh, PA, USA) followed by gel filtration (HiLoad 26/60 Superdex prep grade; GE Healthcare). Endotoxin-free, 0.22- μ m-filtered CL1-R2 batches, suitable for subconjunctival injection in rabbits, were formulated at 10 mg/mL in Dulbecco's phosphate-buffered (D-PBS) solution (pH 7.2) (154 mM NaCl, 10 mM NaPO₄, 2 mM KCl). The solution was stable at -80°C for more than 2 years or at 4°C for up to 6 months. To assess the impact of the crystallizable fragment (Fc) on CNV prevention, Fab'₂ was prepared by digesting 10 mg purified CL1-R2 by using immobilized ficin from the Mouse IgG1 F(ab')₂ Preparation Kit (No. 44980; Pierce, ThermoFisher Scientific, Waltham, MA, USA).

ELB01101 anti-hCD160 mAb was generated by humanization of the parental CL1-R2 mAb by using a modification of the complementarity-determining regions (CDR) grafting approach.³⁰ Humanized ELB01101 was selected for its high affinity for recombinant hCD160 protein (Octet; Fortebio Pall, Pall Corporation, NY, USA) ($K_D \approx 5 \times 10^{-9}$ M) and because it demonstrated a good 50% effective concentration (EC₅₀) when binding the hCD160-transfected E300 cell line. The human IgG4/Km3 κ heavy and light chains of C-terminal-clipped lysine anti-hCD160 ELB01101 were cloned in the pCHO 1.0 plasmid, and ELB01101 was produced by using polyclonal pools of stably transfected Chinese Hamster ovary cells (CHO-S Freedom kit No. A1369601; ThermoFisher Scientific). S228P and R409K mutations were introduced to prevent any "Fab-arm exchange" *in vivo*.^{31,32} ELB01101 was purified from culture supernatants on HiTrap MabSelect SuRe (GE Healthcare) followed by gel filtration (HiLoad 26/60 Superdex 200 prep grade; GE Healthcare) and ion exchange on Sartobind Q, MA15 (Sartorius, Stedim Biotech S.A., Aubagne Cedex, France) in flow-through mode at pH 7.4; it was finally concentrated by using endotoxin-free Vivaspin devices (Sartorius). Highly concentrated (20 mg/mL) ultralow endotoxin (0.025 EU/mg mAb) ELB01101 batches compatible with IVT injection in monkeys were formulated in D-PBS (pH 7.2), sterilized by filtration on a 0.2- μ m membrane (Nalgene; Nunc International, Naperville, IL, USA), aliquoted, and stored at 4°C for up to 1

year. MAb concentrations were determined by absorbance at 280 nm (Nanodrop 2000; ThermoFischer Scientific) and their specific mass extinction coefficients, by using the ProtParam software (Swiss Prot; provided in the public domain by Swiss Institute of Bioinformatics, Geneva, Switzerland, <http://www.expasy.org/>). Endotoxin contamination was verified by using a limulus amoebocyte lysate test (Endosafe PTS; Charles River, Ecully, France). The sequence and molecular integrity of different anti-CD160 mAbs batches were controlled by enzymatic treatment of mAb followed by mass spectrometry analysis of the peptides generated (at the Laboratoire de Spectrométrie de Masse Bio-Organique, UMR 7178 CNRS/University of Strasbourg, France). ELB01101 or the formulation buffer alone as vehicle control was provided as a lipid solution in sterile vials by Elsalys Biotech (Lyon, France) and was stable when stored at 4°C.

The anti-VEGF agents bevacizumab (Avastin; Genentech, San Francisco, CA, USA)—a humanized mAb against all isoforms of VEGF—and aflibercept (Eylea; Bayer Pharmaceuticals, Berlin, Germany)—a fusion protein combining the key binding domains of VEGF receptors 1 and 2 and the Fc portion of immunoglobulin G, which has a high affinity for all isoforms of VEGF and for placental growth factor—were compared to anti-CD160 mAbs in some tests.

Animal Studies and Ethics Statement

Rabbits. A total of 110 male New Zealand albino rabbits (ages 14 ± 1 weeks) were purchased from Charles River (l'Arbresles, France) and used for CNV analyses. Animal care and the study protocol were performed according to the Guide for the Care and Use of Laboratory Animals. During the different trials, animals were housed in individual cages (6400 cm²) and were observed daily. The protocol was approved by the pharmacology, toxicology animal ethics committee at Toulouse University.

Nonhuman Primates. A total of 14 male cynomolgus monkeys (*Macaca fascicularis*) of Chinese origin, obtained from RMS Houston (Houston, TX, USA), were used for laser-induced ChNV studies at Charles River (Senneville, QC, Canada). All of the experimental methods and techniques were conducted in line with the guidelines of the USA National Research Council and the Canadian Council on Animal Care, and complied with the Association for Research in Vision and Ophthalmology's Statement for the Use of Animals in Ophthalmic and Vision Research; the experimental protocol was approved by CR-MTL Institutional Animal Care and Use Committee before its application.

In Vivo Rabbit Corneal Neoangiogenesis Assays

The corneal pocket model was induced by inserting an FGF2- or VEGF-containing lens into rabbit corneas, as previously reported.^{15,16} The approach is fully described elsewhere.³³ All procedures were performed in rabbits under general anesthesia, induced by intramuscular injection of acepromazine (0.75 mg/kg, Calmivet; Vetoquinol, Lure, France), medetomidine (0.25 mg/kg, Dorbene; Laboratorios Syva, Leon, Spain), then ketamine (15 mg/kg, Ketamine 1000; Virbac, Carros, France). An incision was made in the upper region of the cornea, 4 to 5 mm from the limbus. A 1-mm-diameter piece of lens (Lenschatcher GmbH, Dinklage, Germany) soaked with recombinant human FGF2 (500 ng, ref 234-FSE-005; R&D Systems, Minneapolis, MN, USA) or VEGF (500 ng, ref 293-VE-05; R&D Systems) was inserted into this pocket on day 0 (D0). Treatments consisted of two 100- μ g subconjunctival injections in the upper region of the limbus of either CL1-R2 anti-CD160 mAb (30 μ L; Mablife, Evry, France) or control IgG (Ctrl-IgG) (50

μ L). Injections were also performed on anesthetized animals (ketamine 40 mg/kg). These treatments were administered either on D1 and D3 after lens implantation (early treatment) with analysis on D7; or on D6 and D8 after lens implantation (late treatment) and analyzed on D12 (as summarized in Fig. 1A). The same treatment was applied to both eyes in all animals. In some experiments, the effect of CL1-R2 treatment was compared to subconjunctival injection of bevacizumab (100 μ g/50 μ L) or aflibercept (100 μ g/50 μ L). A total of eight animals were used per study, with a minimum of two or three animals treated with IgG control, between two and five animals treated with CL1-R2, and three animals treated with aflibercept or bevacizumab for comparative studies.

CNV Measurements. CNV was graded on a 0-to-4 scale as based on the length of the neovessels formed between the limbus and the lens (see Fig. 1D). CNV was photographed (Canon 550D on binocular microscope, $\times 20$; Canon France, Courbevoie, France) on D1, D3, and D7 or on D6, D8, and D12 to assess the impact of the early and late treatments, respectively. CNV on corneas was manually measured and analyzed by image processing using MorphoExpert software (Explora Nova, La Rochelle, France) to allow quantitative analysis of corneal neovessel length (mm) and count individual neovessels, as well as determining NV area (mm²) (representative images are shown in Fig. 1C).

Evaluation of Additive Effect of CL1-R2 and Anti-VEGF Antibody on Inhibition of CNV in Rabbit. The potential additive effect of combining CL1-R2 and bevacizumab therapy was determined for several groups of rabbits by using the same CNV model. In the monotherapy approach, rabbit groups received two injections of bevacizumab (12.5, 25, 50, or 100 μ g) or CL1-R2 (25, 50, or 100 μ g). In the combination setting, groups were all injected on D1 and D3 with both bevacizumab (25 μ g) and CL1-R2 mAb (doses tested: 25, 50, and 100 μ g) or control IgG1 (25 μ g). A control group injected with IgG1 alone (25 μ g) was also studied. CNV was measured on D7 after lens implantation. Treatment efficacy was expressed as (–) log of (grade obtained with tested dose/grade at dose 0) and plotted as a function of CL1-R2 dose.

Histologic Examination of Formalin-Fixed Rabbit Corneas. Eyeballs were fixed for 48 hours in 10% formalin. After fixing, a circumferential incision was made 2 mm behind the limbus to detach the anterior portion (full cornea plus sclerolimbal ring). The lens implanted in the cornea was identified, and the cornea was bisected in the sagittal plane at 1 mm from the implanted lens (Supplementary Fig. S1). Transversal sections of the cornea were examined after hematoxylin-eosin staining and immunolabeling. The following antibodies were used for immunohistochemistry: anti-caspase 3a (AF835, 1:800, rabbit polyclonal; R&D Systems), anti-Ki-67 (M7240, 1:50, mouse monoclonal; Dakocytomation Dako, Les Ulis, France), anti-CD31 (M0823, 1:20, mouse monoclonal; Dako), anti- α SMA (M0635, 1:25, mouse monoclonal; Dako), and in-house monoclonal anti-CD160 clone 58.1 antibody (tissue culture supernatant ready to use [RTU], courtesy of PB). For staining with the anti-caspase 3 antibody, paraffin-embedded sections were dewaxed in toluene and rehydrated in graded toluene baths, ending with deionized water, before antigen retrieval in EDTA (pH 8) for 30 minutes at 95°C. For the other antibodies, complete pretreatment and antigen retrieval were performed with Dako PTLINK citrate buffer pH 6.0 for 30 minutes in a water bath at 95°C. Cooled sections were then incubated in peroxidase-blocking solution (Dako S2023) to quench endogenous peroxidase activity. To block nonspecific binding, sections were incubated in nonimmune goat serum (Dako X0902, 1:10) for 20 minutes at room temperature (RT). Slides were incubated with primary antibodies for 50 minutes at RT. Secondary antibodies—biotinylated goat anti-mouse immu-

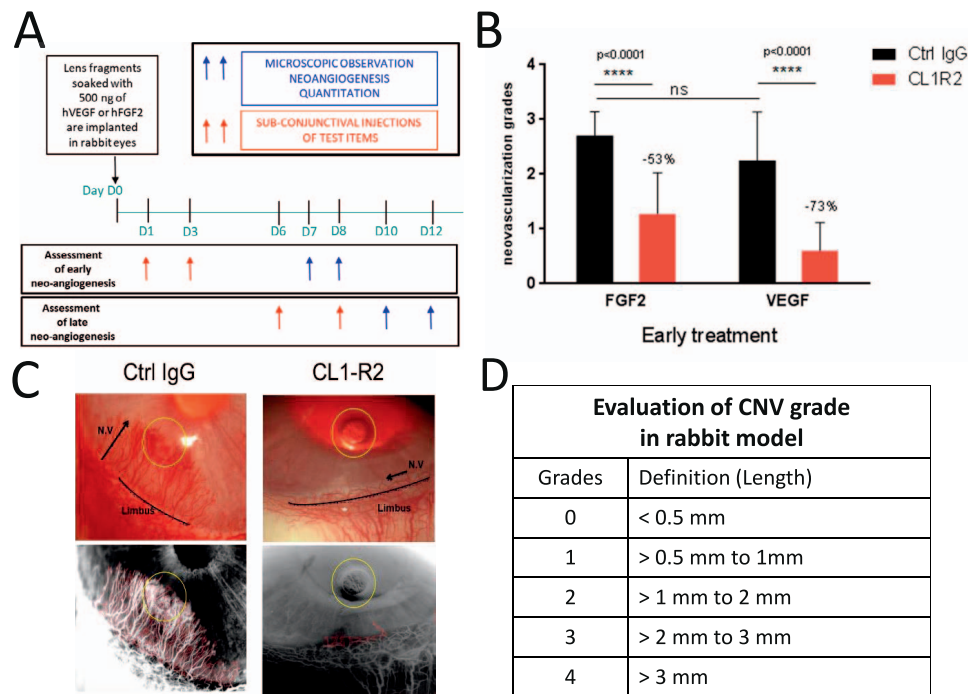


FIGURE 1. CL1-R2 mAb inhibits both FGF2- and VEGF-induced rabbit corneal NV. **(A)** Design of experiments to assess impact of early and late subconjunctival injections of test agents in the CNV rabbit model. **(B)** CL1-R2 mAb inhibits both FGF2- and VEGF-induced rabbit corneal NV. Two subconjunctival injections of either Ctrl-IgG or CL1-R2 (100 µg) were performed on D1 and D3 after implantation of a corneal lens containing either FGF2 or VEGF (early administration). NV grades were determined on D7 after lens implantation, according to a 0- to 4-grade scale. Values correspond to mean ± SD obtained from six independent experiments. *n* = 17 eyes for FGF2/Ctrl-IgG, *n* = 18 for FGF2/CL1-R2, *n* = 8 for VEGF/Ctrl-IgG, *n* = 10 for VEGF/CL1-R2; *****P* < 0.0001, Mann-Whitney *U* test. **(C)** *Top*: Representative images of the NV area and neovessel length originating from the limbus in Ctrl-IgG- and CL1-R2-treated corneas on D12 after FGF2-containing lens implantation (*yellow circles*). *Bottom*: Digital photographs of the same corneas shown at *top* after image processing (MorphoExpert software) to highlight each individual neovessel (in *red*). **(D)** Neovascularization of the cornea in rabbit model was scored at different time points by using a 0- to 4-grade scale.

noglobulins (ABJ125, RTU; ScyTek Laboratories, Inc., West Logan, UT, USA) or swine anti-rabbit immunoglobulins (E0431, 1:200; Dako)—were applied for 25 minutes at RT. Binding was detected with a HRP-streptavidin solution (P0397, 1:500; Dako) for 25 minutes. Peroxidase activity was revealed by using 3, 3'-diaminobenzidine tetrahydrochloride. Micrographs were captured with a Nikon Eclipse Ci microscope equipped with a DS-Fi-1 camera (Nikon, Melville, NY, USA). Images were analyzed with Nis-element AR software.

Preventive Effect of a Single IVT Injection of ELB01101 in Laser-Induced NHP ChNV Model

The ocular tolerance, clinical parameters, and preventive effect of a single IVT injection of 1 mg per eye of the ELB01101 IgG4 mAb or of control vehicle in the laser-induced ChNV model were assessed at Charles River (Senneville, QC, Canada). Standard Charles River procedures were used for this NHP model study; they are described briefly below. Some minor changes were made as compared to the monkey model protocol initially described.^{34,35}

Test and reference compounds were administered by bilateral IVT injection on D0. The target dose volume for each animal was 50 µL/eye, corresponding to 1 mg of compound. The doses were delivered with a 1-mL syringe and an Exelint U-100 insulin 0.5-mL syringe (Exelint International Co., CA, USA) fitted with a 29 gauge × ½-inch needle. On D1 a 9-spot laser wound pattern was successfully created in both eyes in six animals per group. The pattern was located between the major retinal vessels, around the area of the macula in each eye, and was produced by using an 810-nm diode laser at an initial

power setting of 300 mW, an initial spot size of 80 µm, and with a pulse duration of 0.1 seconds. A total of 108 laser sites/group were assessed for each treatment (six animals/group, two eyes/animal, nine sites/eye for each treatment to be tested). The development of active ChNV lesions from the individual laser spots on the still images was assessed by fluorescein angiography (FA) before injury and on D1, D14, and D29 after laser injury. ChNV lesions were semiquantitatively evaluated to assess leakage and were graded on a scale from 0 to 4 by two experienced independent blinded readers, who subsequently determined a consensus score by using the following scale: grade 0, no leakage; grade 1, minimal leakage; grade 2, slight leakage; grade 3, moderate leakage (semisolid to solid hyperfluorescence generally remaining within the boundary of the laser-induced defect); and grade 4, substantial leakage (solid hyperfluorescent region extending beyond the boundary of the laser-induced defect). The number of clinically relevant lesions was defined by combining grade-3 and grade-4 lesions. The incidence of treatment on clinically relevant lesions was expressed as the incidence rate—defined as the number of clinically relevant lesions that occurred during a given interval—divided by the total number of lesions induced (incidence rate could also be expressed as a percentage). The incidence rate ratio (IRR),²⁷ which refers to the ratio of the incidence rate of clinically relevant lesions in treated eyes to the incidence rate in control eyes, was determined. An IRR much smaller than 1 indicates a reduction in the incidence of clinically relevant lesions in the treated group versus the control group. Animals were observed once in the morning and once in the afternoon. Food consumption was recorded. Detailed examinations, including weighing, were performed

weekly. Ophthalmic examinations (funduscopy: direct and indirect ophthalmoscopy, and slit lamp analysis) were performed once before laser induction (control exam) and after laser induction on D9 and D28.

Statistical Analysis

Statistical analyses were performed by using GraphPad Prism software (version 6; GraphPad, San Diego, CA, USA). Differences in NV grades, length, and area between the experimental and control groups were analyzed by using Mann-Whitney tests. Results are presented as mean \pm SD. The threshold for statistical significance was set at 0.05. The significance of *P* values is indicated in all figure legends. To determine the statistical significance of percentage differences of clinically relevant lesions between the vehicle control group and ELB01101 in the ChNV NHP model, a χ^2 test was performed.

RESULTS

Early Administration of Anti-CD160 CL1-R2 in Rabbits Inhibits Both FGF2- and VEGF-Mediated CNV

The results presented in Figure 1B show a significant decrease in neovascular growth after treatment with CL1-R2 (53% and 73% reduction after FGF2 and VEGF induction, respectively). As compared to the Ctrl-IgG group, early subconjunctival administration of CL1-R2 mAb on D1 and D3 after corneal implantation of lens resulted in statistically significant inhibition of CNV scored on D7; the degree of NV in animals from both groups was equivalent before treatment. NV levels were statistically similar when comparing FGF2 and VEGF treatments. No adverse ocular complications related to subconjunctival injection were observed (data not shown).

Digital photographs of cornea were analyzed by image processing to record changes in CNV (representative images are shown in Fig. 1C). This analysis demonstrated a strong inhibition of corneal NV after treatment with CL1-R2 compared to vehicle control. Significant strong inhibition of NV area and length of neovessels emerging from the limbus was observed in CL1-R2-treated corneas compared to the Ctrl-IgG-treated corneas on D12 after implantation of FGF2-containing lenses (Fig. 1C, lower panel).

Late Administration of Anti-CD160 CL1-R2 Has a Significant Antiangiogenic Effect on CNV, Equivalent to That Seen With Bevacizumab or Aflibercept

Administering CL1-R2 mAb on D6 and D8 post implantation (late treatment) resulted in statistically significant inhibition of CNV, as scored on D12, compared to treatment with Ctrl-IgG (Fig. 2). Treatment with CL1-R2 was compared to two reference treatments, bevacizumab and aflibercept (Fig. 2A). In the same administration conditions, although the intensity of decrease observed on D12 after each treatment varied (very high after aflibercept treatment, high after CL1-R2, and lower after bevacizumab), both CL1-R2 and aflibercept decreased NV length (Fig. 2B) and NV area (Fig. 2C). However, the aflibercept-mediated inhibition of CNV and NV areas was significantly faster than that observed with CL1-R2 treatment (45% inhibition with CL1-R2 versus 84% inhibition with aflibercept) (Fig. 2C). Late treatment with CL1-R2 therefore had a slower antiangiogenic effect than aflibercept (Figs. 2B, 2C).

Strong Antiangiogenic Properties Confirmed by Histologic and Immunohistochemical Analysis Along With Regression of CNV Following Late CL1-R2 Treatment

Histologic examinations of corneal and limbus tissue sections (Figs. 3, 4 respectively) were performed 10 to 12 days after implantation of FGF2-containing lens (late Ctrl-IgG or CL1-R2 treatment administered on D6 and D8). Expression was analyzed for the following markers: CD160, CD31 (vascular marker of endothelium of corneal vessels), α SMA (marker of pericytes covering differentiated vessels and myofibroblasts), and Ki-67 (marker of proliferating cells). Examination of IgG control groups confirmed neovessel invasion of the cornea toward the lens pocket, forming a medium- to high-density vascular network, of variable diameter, in the superficial third of the corneal stroma. CD31 and α SMA labeling were consistent with mature functional vessels containing red blood cells in their vascular lumens (Figs. 3A, 3C). In contrast, corneas from CL1-R2-treated groups showed no vascularization or only focal, rare, and small-caliber neovessels (Figs. 3B, 3D). The persistence of CD31 and α SMA labeling highlighted the mature status of these residual vessels. Endothelial proliferation of growing neovessels was mostly observed with samples from IgG groups. In the CL1-R2 groups, some of the residual neovessels also contained a few Ki-67-positive cells, suggesting that neovascularization resumed after discontinuing the antiangiogenic treatment (Fig. 3). CD160 labeling was stable and similar in corneal (Figs. 4A, 4B) and limbal (Figs. 4C, 4D) neovessels in both IgG- and CL1-R2-treated samples, with labeling of the endothelial lining (Fig. 4). After CL1-R2 treatment, proliferative limbic vessels with open lumen were comparable to those observed in the IgG-treated group. No caspase reactivity was recorded.

FGF2-Induced Rabbit CNV Inhibited by the CL1-R2 mAb as IgG or Fab'2

The effects of CL1-R2 as a whole IgG and in Fab'2 formats on progression of CNV were compared to those of bevacizumab and a control murine IgG1 in the same model (Fig. 5). The anti-CD160 mAb as a whole IgG and as a Fab'2 fragment inhibited NV significantly better than control IgG1, and controlled NV to a roughly equivalent extent to the commercial form of bevacizumab. The Fab'2 form of CL1-R2 is as potent, or even better, for NV inhibition as its whole IgG form, but this difference could be explained by the fact that Fab'2 and whole IgG were used in equivalent amounts by weight rather than at equivalent molarity (which corresponds to 1.5-fold more active product for the Fab'2 form).

CD160-Mediated Pathway Additively Combines With VEGF/VEGFR2 Pathway to Inhibit CNV in a Rabbit Model

In the rabbit model, we also examined how CNV evolved upon inhibition of the VEGF/VEGFR pathway by using a suboptimal dose of bevacizumab in combination with increasing doses of anti-CD160 mAb (Figs. 6C, 6D). Preliminary results showed that 100 μ g bevacizumab almost completely abolished CNV in this model (Fig. 6A). For this study, we therefore selected the suboptimal dose of 25 μ g bevacizumab in combination with CL1-R2 at a starting suboptimal dose of 25 μ g and which was also administered at 50 and 100 μ g. At 25 μ g, bevacizumab appeared to be slightly more potent than CL1-R2 in controlling CNV (50% bevacizumab alone versus 25% CL1-R2 in Figs. 6B, 6C, respectively). However, both single mAb treatments were

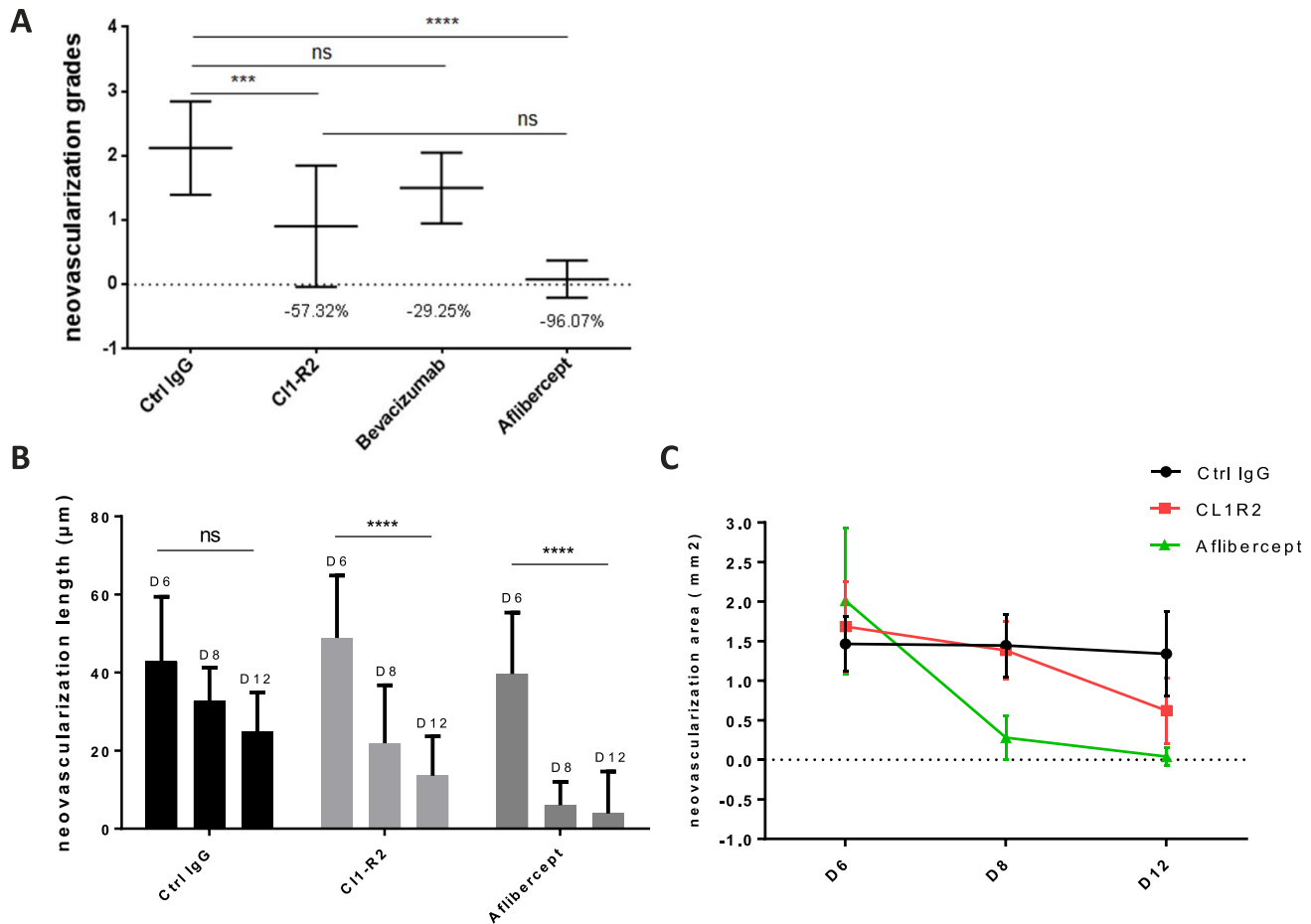


FIGURE 2. CL1-R2 mAb, bevacizumab, and aflibercept inhibit FGF2-induced late corneal NV. (A) Two subconjunctival injections of Ctrl-IgG, CL1-R2, or bevacizumab (100 µg/50 µL each) were performed on D6 and D8 after implantation of a corneal lens containing FGF2 (late administration). NV was graded on D10 or D12, as described for Figure 1D. Values correspond to mean ± SD obtained from two independent experiments, $n = 17$ eyes for Ctrl-IgG and CL1-R2, $n = 6$ for bevacizumab; **** $P < 0.0001$; * $P < 0.01$. (B, C) Corneas were treated by subconjunctival injections of Ctrl-IgG, CL1-R2, or aflibercept (100 µg/50 µL each) on D6 and D8 after lens implantation. Corneal NV length (B) and corneal NV areas (C) were evaluated by image processing on D6, D8, and D12. Values correspond to mean ± SD obtained from two independent experiments, $n = 16$ eyes for Ctrl-IgG, $n = 10$ for CL1-R2, $n = 12$ for aflibercept; **** $P < 0.0001$. NS, not significant.

equally potent at the 50- and 100-µg doses (see Figs. 6A, 6B). The capacity of the combination to control CNV increased with the dose of CL1-R2 added (Fig. 6C, and as shown by the linearity of response in Fig. 6D). The results shown in Figures 6C and 6D indicated that early treatment with CL1-R2 along with an anti-VEGF antibody provided better NV inhibition in an ocular neovascularization model than either antibody alone.

A Single IVT Injection of ELB01101 Has a Preventive Effect in Laser-Induced NHP ChNV Model

The objective of this part of our study was to determine both the safety and efficacy of ELB01101 in a relevant simian model.

ELB01101 Safety Assessment. Clinical and ophthalmologic examinations revealed no significant treatment-related effects in terms of bleeding, body weight, or macroscopic findings. The minor effects observed were considered incidental or procedure related and typical of laboratory-housed primates. Laser exposure resulted in similar procedure-related ocular changes in all treated eyes, including retinal scarring, hemorrhages, and foveal hemorrhages. The chorioretinal hemorrhages improved over time and had resolved in most eyes by D28. Very slight cell-like opacities in the anterior

portion of the vitreous were noted on D28 in 9 of 12 eyes treated with 1 mg ELB01101. These cells were also observed bilaterally on D9 and D28 in one of the control animals treated with D-PBS.

Fluorescein Angiography Results. The results of FA evaluation are presented in Figures 7A and 7B, and representative FA images are shown in Figure 7C for both groups. The number of clinically relevant lesions (grade 3: moderate leakage and grade 4: substantial leakage; combined) was greater in the vehicle group on D14 and D29. On D14, ELB01101 had a better preventive effect on ChNV than the vehicle control (only 10.2% of clinically relevant lesions with ELB01101 compared to 15.7% with vehicle control, χ^2 test, $P = 0.2242$; χ^2 statistic = 1.4772). Unfortunately, this effect was not significant (Figs. 7A, 7B). On D29, the difference between the percentage of clinically relevant lesions recorded in ELB01101-treated animals compared to control-treated animals was statistically significant (12% with ELB01101 versus 23.1% with vehicle control; $P = 0.032001$, χ^2 statistic = 4.5985). Also on D29, an incidence rate for clinically relevant lesions relative to the total number of laser spots of 0.12 (13 of 108) was determined for eyes treated with ELB01101, as compared to 0.231 (25 of 108) for the vehicle group. The corresponding IRR was 0.519; this value should be compared to the IRR reported

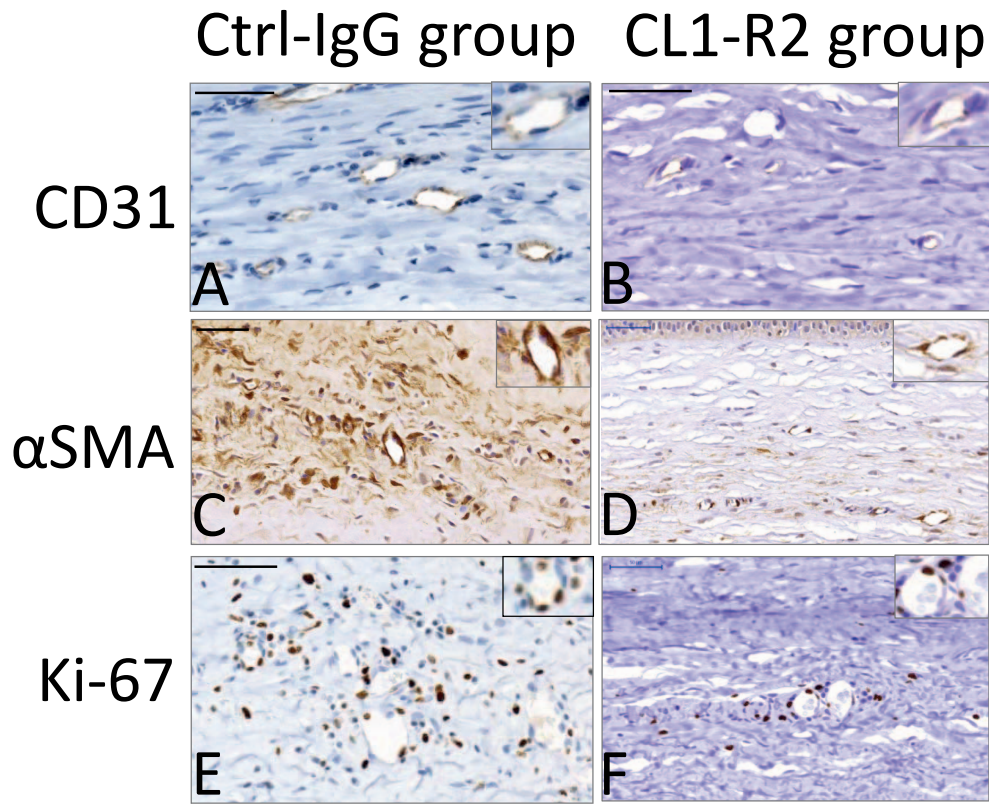


FIGURE 3. Immunohistochemical analysis of corneal neovessels in Ctrl-IgG-treated group (*left*) and CL1-R2-treated group (*right*): the dense vascular network (Ctrl-IgG group) and residual small vessels (CL1-R2 group) were both labeled with CD31 (A, B) and αSMA (C, D) antibodies. Proliferating Ki-67-stained endothelial cells were frequently observed in samples from the IgG group (E) and more rarely in residual vessels from the CL1-R2 group (F). Some perivascular inflammatory cells were also labeled with Ki-67. *Scale bar*: 50 μm. On D10 after lens implantation, corneal tissue sections were stained with anti-αSMA, CD31, and Ki-67 mAbs and photographed (Canon 550D on binocular microscope).

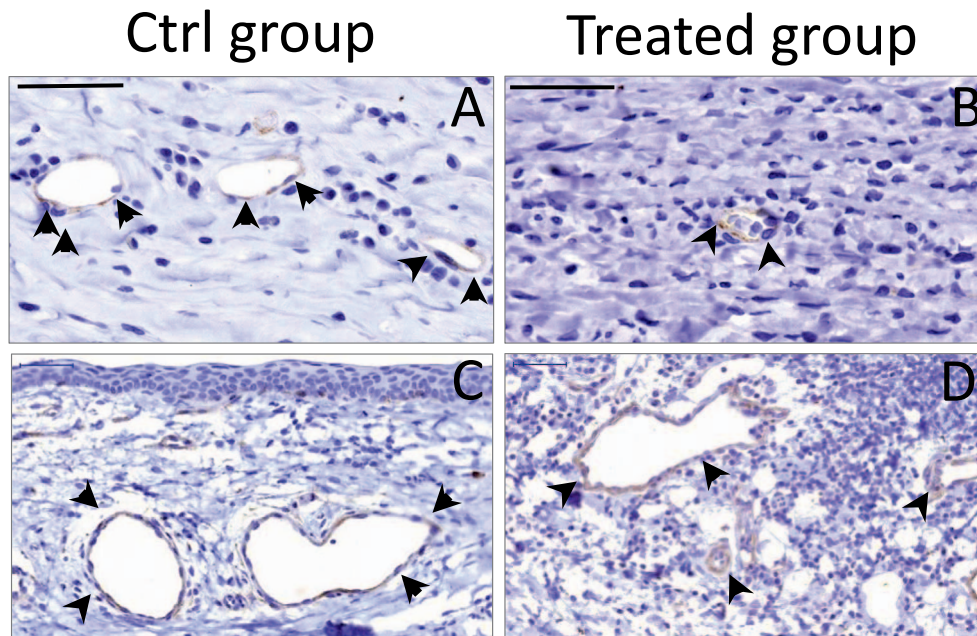


FIGURE 4. Immunohistochemical analysis of CD160 expression in cornea and limbus. Anti-CD160 immunohistochemistry revealed persistent CD160 labeling of endothelial cells in cornea (A, B) and limbus (C, D) from the Ctrl-IgG group (A, C) and the CL1-R2 group (B, D), indicated by the *brown staining* highlighting the vessel wall (*arrowheads*). (A-C) *Scale bar*: 50 μm. (D) *Scale bar*: 100 μm.

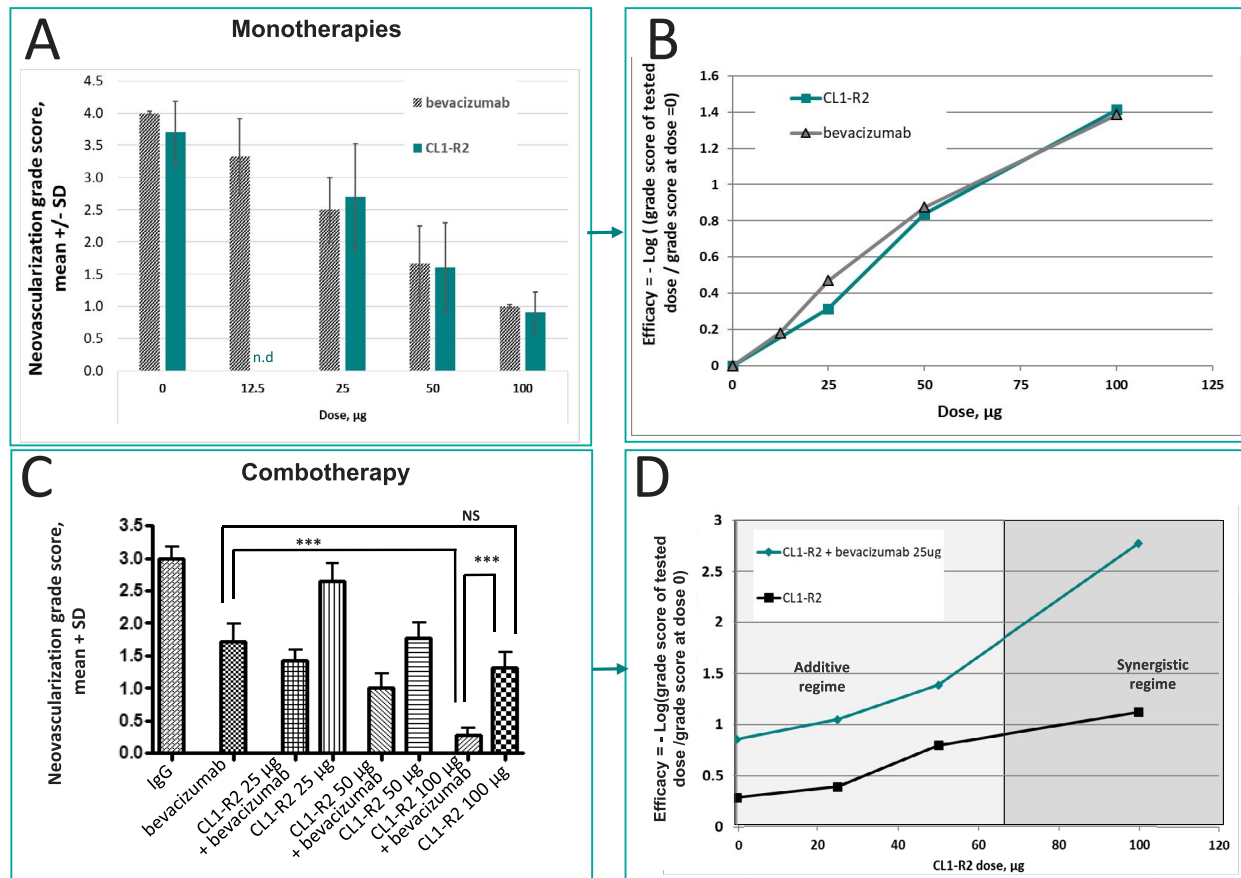


FIGURE 6. CL1-R2 and anti-VEGF antibody have an additive effect when used in combination to inhibit CNV in rabbit. **(A)** Dose-response for each group in the rabbit CNV model treated by monotherapy. On D1 and D3 after implantation of FGF2-containing lens, groups of rabbits were given two subconjunctival injections of bevacizumab (12.5, 25, 50, or 100 μg) or CL1-R2 (12.5 [not done, n.d.], 25, 50, or 100 μg). NV was graded on D7 after lens implantation. Mean ± SD of the neovascularization grade score is reported. $n = 6$ for bevacizumab and $n = 12$ for CL1-R2. **(B)** The efficacy of each monotherapy was expressed as $(-)$ log of (grade obtained with tested dose/grade at dose 0) and plotted as a function of dose. **(C)** Dose-response in rabbit CNV model following combination therapy. Rabbits were all injected on D1 and D3 with bevacizumab (one injection of 25 μg) in combination with different doses (25, 50, and 100 μg) of the anti-CD160 CL1-R2 mAb; a control group was also treated with the Ctrl-IgG alone (25 μg). CNV was measured on D7 after lens implantation, as described. $n = 9$ to 16 for each experimental condition. **(D)** The efficacy of anti-CD160 CL1-R2 in monotherapy or in combination with bevacizumab was compared by expressing the efficacy as $(-)$ log of (grade obtained with tested dose/grade at dose 0) for each condition, and the efficacies calculated were plotted as a function of the CL1-R2 dose.

bevacizumab. Bevacizumab appeared to be slightly more potent than either CL1-R2 format, but this difference could be explained by the fact that this murine CL1-R2 has not been optimized for affinity for its target or formatted or formulated as a therapeutic antibody. When late treatment of CL1-R2 was compared to bevacizumab or to aflibercept, all treatments led to a significant decrease in both CNV area and neovessel length, although treatment with CL1-R2 acted less rapidly than aflibercept.

Immunohistochemical studies confirmed that late treatment with CL1-R2 induced significant regression of neovessels expressing CD31, aSMA, and Ki-67, indicating that anti-CD160 therapy clearly controls the appearance of newly formed corneal blood vessels. aSMA labeling could be explained by a certain number of neovessels that undergo maturation, involving coverage of corneal endothelial cells by pericytes expressing the aSMA marker (as described in the study by Cursiefen et al.⁴⁶). Thus, the compilation of these data indicated that anti-CD160 mAb controls both early and late neovascularization.

To produce a therapeutic anti-human CD160 compatible with formulation constraints for IVT injections, we generated a novel anti-hCD160 by CDR grafting from CL1-R2. The resulting

humanized ELB01101 was in the form of a reduced Fcγ receptor IgG4-binder. After selection, the affinity of ELB01101 for hCD160 was unexpectedly found to be improved 3-fold (K_D , 4×10^{-9} nM; data not shown) during the humanization process. The antibody was very stable at 4°C and RT, resistant to low pH, and soluble even at high concentrations.

Administration of the novel anti-CD160 ELB01101 mAb, by single bilateral IVT injection of 1 mg in cynomolgus laser-induced ChNV eyes, was very well tolerated, both locally and systemically. Thus, its safety profile in terms of ocular inflammation was good, confirming observations from previous studies (a pharmacokinetic study in which 500 μg CL1-R2 was intravenously (IV) and IVT injected in New Zealand rabbits or during a previous ocular tolerability study in NHP, using a 1-mg dose of different isoforms of humanized anti-CD160 including ELB01101 and ELB01111 [the same variable regions of ELB01101 formatted as an IgG1 N297Q/κ antibody]; data not shown). Ophthalmologic examinations in this study revealed very slight cell-like vitreal opacities on D28 in animals treated with ELB01101 (a similar effect was observed when testing the ocular tolerance of ELB01101 on D7 post-IVT injection in a non-laser-treated eye). However, these incidents were not considered clinically important because this type of

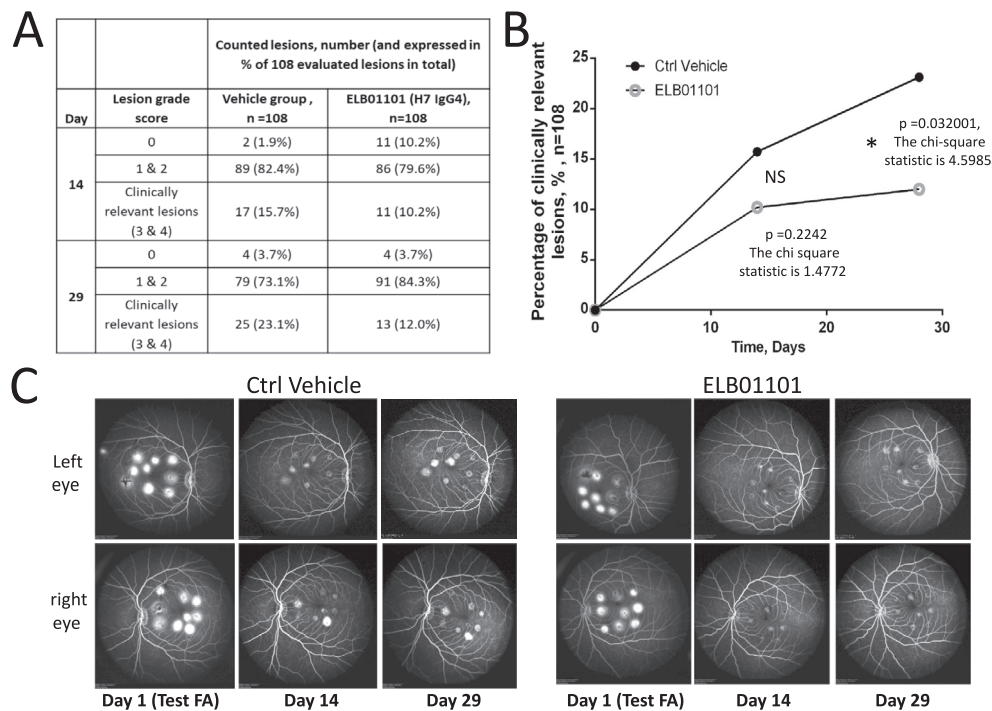


FIGURE 7. ELB01101 prevents the incidence of clinically relevant lesions in a laser-induced ChNV NHP model and increases the number of healing lesions. (A) Table summarizing the incidence of treatments based on grade of laser-induced lesions (0, 1 + 2, or clinically relevant lesions [corresponding to grades 3 and 4]), as presented graphically in (B), expressed either as a total number or as a percentage of total lesions. The total number of laser-induced lesions was 108 for each group of animals treated with ELB01101 anti-CD160 (H7 IgG4) or vehicle control (12 eyes, nine laser impacts per eye). (B) Comparison of incidence of one intravitreal administration of anti-CD160 ELB01101 IgG4 or vehicle control on percentage of clinically relevant lesions (scores 3 and 4 out of the 108 initial laser impacts). D29: the χ^2 statistic is 4.5985; $P = 0.032001$. D14: not significant, the χ^2 statistic is 1.4772; $P = 0.224213$. (C) Representative fluorescein angiography images for Ctrl vehicle- and ELB01101-treated groups at Day 1 (postlaser), Day 14, and Day 29.

change is commonly observed with IVT drug administration. Furthermore, similar transient cells in the vitreous and anterior chamber were also observed with vehicle control and in previous studies with ranibizumab injection in monkeys (either alone²⁷ or in combination with verteporfin²⁶). In these previous studies, these inflammatory symptoms resolved with time and were reduced with subsequent injections.

The anti-CD160 monoclonal antibodies used here were developed for use in combination with anti-VEGF therapies, not as an alternative standard of care, except for use in patients refractory to anti-VEGF therapies. Even if combination therapy is the objective, the efficacy of the mAbs as monotherapy must be demonstrated in a relevant animal model.

This study was designed to answer this question as a first demonstration of tolerability/efficacy in a relevant animal model with the first generation of anti-CD160 therapy.

Results showed the incidence of ChNV, defined angiographically, to be significantly lower on D29 in eyes treated with 1 mg ELB01101 than in eyes treated with vehicle control ($P = 0.032001$). However, comparison of ELB01101 efficacy in the simian ChNV model with literature data (versus efficacy of ranibizumab as reported in the studies by Husain et al.²⁶ and Krzystolik et al.²⁷; of bevacizumab, by Lichtlen et al.²⁸; and of aflibercept, by Nork et al.²⁹) indicated that this dose of ELB01101 is not as effective as anti-VEGFs for full control of ChNV. It was therefore necessary to improve the efficacy of ELB01101 through the production of a second generation of more potent anti-CD160 mAbs (following affinity maturation for ELB01101). This second generation was designed on backbone formats of mAb and mAb fragments that improve the pharmacoki-

netic parameters of leads (e.g., by improving the residence time in the eye and allowing a higher ratio of residence time in the eye over systemic exposure, as described in the study of Gadkar et al.⁴⁷). This new generation of anti-CD160 mAbs is currently being tested to determine dose-range efficacy in the ChNV NHP model in a preventive setting, and the efficacy of a combination of anti-CD160 mAbs with Lucentis versus each monotherapy is being studied in a therapeutic setting. This first proof of concept in a relevant NHP model indicates that CD160 significantly contributes to the formation of ChNV lesions, and as a result, the development of a therapeutic anti-CD160 antibody for use in combination with anti-VEGF therapy to treat choroidal and retinal neovascular ocular diseases is highly relevant.

The fact that early subconjunctival administration of CL1-R2 inhibited both FGF2- and VEGF-induced CNV in a similar manner favors a VEGF-independent mode of action of the CD160 pathway. However, the FGF2 and VEGF pathways are unlikely to be completely independent, particularly in vivo. The synergy between the CD160 and VEGF pathways was demonstrated by the fact that, when anti-CD160 was tested in combination with bevacizumab in the CNV rabbit model, CNV was inhibited to a greater extent at all anti-CD160 doses tested. These two pathways may therefore act in an additive manner. The finding that both CD160 and VEGF pathways contribute to the efficacy observed implies that the anti-CD160 from the ELB01101 program acts differently from currently available anti-VEGFs. These results indicate that anti-CD160 and anti-VEGF therapies could be highly useful in combination for the treatment of neovascular eye diseases.

CONCLUSIONS

In the primate ChNV model, ELB01101 mAb was well tolerated at 1 mg/eye throughout the experiment, and treatment with anti-CD160 prevented the incidence of around 50% of clinically relevant lesions on D29 as compared to the vehicle control treatment. This result validates and confirms the safety of targeting CD160 when treating retinal diseases in the most relevant animal model of wAMD. The results obtained with ELB01101 IgG4 mAb pave the way for tests of a new generation of more potent anti-CD160 leads with longer local residence times that could potentialize the current standard of care, or be used as alternative therapies in subpopulations of anti-VEGF-resistant patients, or patients with refractory neovascular AMD or diabetic macular edema (DME).

Interestingly, the additive effect observed upon treatment with CL1-R2 in combination with bevacizumab in the CNV rabbit model suggests that both CD160 and VEGF pathways contribute to the efficacy observed, and that the two mAbs probably act via different pathways. This could result in new therapeutic opportunities for cotargeted or combination therapies alongside anti-VEGFs.

Acknowledgments

The authors thank Maryse Aguerre-Girr, Marie-Andrée Daussion, Jeanine Boyes, Benjamin Gil, and Julie Tabiasco for their assistance in preparing and contributing to some of the experiments and various aspects of this study, and Pascal Clerc for assistance with analysis of MorphoExpert data. The English language was edited by Maighread Gallagher, PhD (TWS Editing).

Supported in part by INSERM, CNRS, Toulouse III University, Association Valentin Haüy, and through Grant ANR-12-RPIB-0009 from the French National Agency for Research. The funders played no role in study design, data collection and analysis, decision to publish, or preparation of the manuscript.

Disclosure: **T. Menguy**, Elsalsys Biotech (E), P; **A. Briaux**, None; **E. Jeunesse**, None; **J. Giustiniani**, None; **A. Calcei**, Elsalsys Biotech (E), P; **T. Guyon**, None; **J. Mizrahi**, Elsalsys Biotech (C); **H. Haegel**, Elsalsys Biotech (E), P; **V. Duong**, Elsalsys Biotech (E); **V. Soler**, None; **P. Brousset**, None; **A. Bensussan**, P; **I. Raymond Letron**, None; **P. Le Bouteiller**, P

References

- Carmeliet P, Jain RK. Principles and mechanisms of vessel normalization for cancer and other angiogenic diseases. *Nat Rev Drug Discov*. 2011;10:417-427.
- Sherris D. Ocular drug development: future directions. *Angiogenesis*. 2007;10:71-76.
- World Health Organization. *Prevention of Blindness and Visual Impairment: Priority Eye Diseases*. Geneva, Switzerland: WHO; 2016.
- World Health Organization. *Global Data on Visual Impairments: 2010*. Geneva, Switzerland: WHO; 2012.
- Solomon SD, Lindsley K, Vedula SS, et al. Anti-vascular endothelial growth factor for neovascular age-related macular degeneration. *Cochrane Database Syst Rev*. 2014;8:CD005139.
- Dhoot DS, Avery RL. Vascular endothelial growth factor inhibitors for diabetic retinopathy. *Curr Diab Rep*. 2016;16:122.
- Fletcher EC, Chong NV. Looking beyond Lucentis on the management of macular degeneration. *Eye Lond Engl*. 2008;22:742-750.
- Ferrara N, Adamis AP. Ten years of anti-vascular endothelial growth factor therapy. *Nat Rev Drug Discov*. 2016;15:385-403.
- Rosenfeld PJ, Brown DM, Heier JS, et al. Ranibizumab for neovascular age-related macular degeneration. *N Engl J Med*. 2006;355:1419-1431.
- Heier JS, Brown DM, Chong V, et al. Intravitreal aflibercept (VEGF trap-eye) in wet age-related macular degeneration. *Ophthalmology*. 2012;119:2537-2548.
- Yang S, Zhao J, Sun X. Resistance to anti-VEGF therapy in neovascular age-related macular degeneration: a comprehensive review. *Drug Des Devel Ther*. 2016;10:1857-1867.
- Carneiro AM, Costa R, Falcão MS, et al. Vascular endothelial growth factor plasma levels before and after treatment of neovascular age-related macular degeneration with bevacizumab or ranibizumab. *Acta Ophthalmol*. 2012;90:e25-e30.
- Zehetner C, Kirchmair R, Huber S, et al. Plasma levels of vascular endothelial growth factor before and after intravitreal injection of bevacizumab, ranibizumab and pegaptanib in patients with age-related macular degeneration, and in patients with diabetic macular oedema. *Br J Ophthalmol*. 2013;97:454-459.
- Wang X, Sawada T, Sawada O, et al. Serum and plasma vascular endothelial growth factor concentrations before and after intravitreal injection of aflibercept or ranibizumab for age-related macular degeneration. *Am J Ophthalmol*. 2014;158:738-744.e1.
- Fons P, Chabot S, Cartwright JE, et al. Soluble HLA-G1 inhibits angiogenesis through an apoptotic pathway and by direct binding to CD160 receptor expressed by endothelial cells. *Blood*. 2006;108:2608-2615.
- Chabot S, Jabrane-Ferrat N, Bigot K, et al. A novel antiangiogenic and vascular normalization therapy targeted against human CD160 receptor. *J Exp Med*. 2011;208:973-986.
- Abecassis S, Giustiniani J, Meyer N, et al. Identification of a novel CD160+ CD4+ T-lymphocyte subset in the skin: a possible role for CD160 in skin inflammation. *J Invest Dermatol*. 2007;127:1161-1166.
- Anumanthan A, Bensussan A, Boumsell L, et al. Cloning of BY55, a novel Ig superfamily member expressed on NK cells, CTL, and intestinal intraepithelial lymphocytes. *J Immunol*. 1998;161:2780-2790.
- Nikolova M, Marie-Cardine A, Boumsell L, Bensussan A. BY55/CD160 acts as a co-receptor in TCR signal transduction of a human circulating cytotoxic effector T lymphocyte subset lacking CD28 expression. *Int Immunol*. 2002;14:445-451.
- Zuo J, Shan Z, Zhou L, et al. Increased CD160 expression on circulating natural killer cells in atherosclerosis. *J Transl Med*. 2015;13:188.
- Ortonne N, Ram-Wolff C, Giustiniani J, et al. Human and mouse mast cells express and secrete the GPI-anchored isoform of CD160. *J Invest Dermatol*. 2011;131:916-924.
- Barman S, Kayama H, Okuzaki D, et al. Identification of a human intestinal myeloid cell subset that regulates gut homeostasis. *Int Immunol*. 2016;28:533-545.
- Giustiniani J, Marie-Cardine A, Bensussan A. A soluble form of the MHC class I-specific CD160 receptor is released from human activated NK lymphocytes and inhibits cell-mediated cytotoxicity. *J Immunol*. 2007;178:1293-1300.
- Chen W-L, Chen Y-M, Chu H-S, et al. Mechanisms controlling the effects of bevacizumab (avastin) on the inhibition of early but not late formed corneal neovascularization. *PLoS One*. 2014;9:e94205.
- Kim EK, Kong SJ, Chung SK. Comparative study of ranibizumab and bevacizumab on corneal neovascularization in rabbits. *Cornea*. 2014;33:60-64.
- Husain D, Kim I, Gauthier D, et al. Safety and efficacy of intravitreal injection of ranibizumab in combination with verteporfin PDT on experimental choroidal neovascularization in the monkey. *Arch Ophthalmol*. 2005;123:509-516.

27. Krzystolik MG, Afshari MA, Adamis AP, et al. Prevention of experimental choroidal neovascularization with intravitreal anti-vascular endothelial growth factor antibody fragment. *Arch Ophthalmol*. 2002;120:338-346.
28. Lichtlen P, Lam TT, Nork TM, et al. Relative contribution of VEGF and TNF-alpha in the cynomolgus laser-induced CNV model: comparing the efficacy of bevacizumab, adalimumab, and ESBA105. *Invest Ophthalmol Vis Sci*. 2010;51:4738-4745.
29. Nork TM, Dubielzig RR, Christian BJ, et al. Prevention of experimental choroidal neovascularization and resolution of active lesions by VEGF trap in nonhuman primates. *Arch Ophthalmol*. 2011;129:1042-1052.
30. Jones PT, Dear PH, Foote J, et al. Replacing the complementarity-determining regions in a human antibody with those from a mouse. *Nature*. 1986;321:522-525.
31. Angel CA, Pringle JH, Primrose L, Lauder I. Detection of immunoglobulin heavy chain gene rearrangements in Hodgkin's disease using PCR. *J Clin Pathol*. 1993;46:940-942.
32. Labrijn AF, Rispens T, Meesters J, et al. Species-specific determinants in the IgG CH3 domain enable Fab-Arm exchange by affecting the noncovalent CH3-CH3 interaction strength. *J Immunol*. 2011;187:3238-3246.
33. Morbidelli L, Ziche M. The rabbit corneal pocket assay. *Methods Mol Biol*. 2016;1430:299-310.
34. Ohkuma H, Ryan SJ. Vascular casts of experimental subretinal neovascularization in monkeys: a preliminary report. *Jpn J Ophthalmol*. 1982;26:150-158.
35. Ryan SJ. Subretinal neovascularization: natural history of an experimental model. *Arch Ophthalmol*. 1982;100:1804-1809.
36. Dunn EN, Hariprasad SM, Sheth VS. An overview of the Fovista and Rinucumab trials and the fate of anti-PDGF medications. *Ophthalmic Surg Lasers Imaging Retina*. 2017;48:100-104.
37. Saharinen P, Eklund L, Alitalo K. Therapeutic targeting of the angiopoietin-TIE pathway. *Nat Rev Drug Discov*. 2017;16:635-661.
38. Kojima R, Kajikawa M, Shiroishi M, et al. Molecular basis for herpesvirus entry mediator recognition by the human immune inhibitory receptor CD160 and its relationship to the cosignaling molecules BTLA and LIGHT. *J Mol Biol*. 2011;413:762-772.
39. El-Far M, Pellerin C, Pilote L, et al. CD160 isoforms and regulation of CD4 and CD8 T-cell responses. *J Transl Med*. 2014;12:217.
40. Sakoda Y, Anand S, Zhao Y, et al. Herpesvirus entry mediator regulates hypoxia-inducible factor-1 α and erythropoiesis in mice. *J Clin Invest*. 2011;121:4810-4819.
41. Chen L-J, Ito S, Kai H, et al. Microfluidic co-cultures of retinal pigment epithelial cells and vascular endothelial cells to investigate choroidal angiogenesis. *Sci Rep*. 2017;7:3538.
42. Bechill J, Müller WJ. Herpesvirus entry mediator (HVEM) attenuates signals mediated by the lymphotoxin β receptor (LT β R) in human cells stimulated by the shared ligand LIGHT. *Mol Immunol*. 2014;62:96-103.
43. Chang YH, Hsieh SL, Chao Y, et al. Proinflammatory effects of LIGHT through HVEM and LT β R interactions in cultured human umbilical vein endothelial cells. *J Biomed Sci*. 2005;12:363-375.
44. Gopalakrishnan V, Purushothaman P, Bhaskar A. Proteomic analysis of plasma proteins in diabetic retinopathy patients by two dimensional electrophoresis and MALDI-Tof-MS. *J Diabetes Complications*. 2015;29:928-936.
45. Henry A, Boulagnon-Rombi C, Menguy T, et al. CD160 expression in retinal vessels is associated with retinal neovascular diseases. *Invest Ophthalmol Vis Sci*. 2018;59:2679-2686.
46. Cursiefen C, Hofmann-Rummelt C, Kuchle M, Schlötzer-Schrehardt U. Pericyte recruitment in human corneal angiogenesis: an ultrastructural study with clinicopathological correlation. *Br J Ophthalmol*. 2003;87:101-106.
47. Gadkar K, Pastuskovas CV, Le Couter JE, et al. Design and pharmacokinetic characterization of novel antibody formats for ocular therapeutics. *Invest Ophthalmol Vis Sci*. 2015;56:5390-5400.